REPRESENTATION OF UNKNOWN PARAMETERS IN GEOTHERMAL MODEL CALIBRATION

Ruanui Nicholson[1], Oliver J. Maclaren[1], John P. O'Sullivan[1], Michael J. O'Sullivan[1], Anna Suzuki[2] and Elvar K. Bjarkason[2]

[1]Department of Engineering Science, The University of Auckland, Auckland 1142, New Zealand

[2]Institute of Fluid Science, Tohoku University, Sendai, Japan

ruanui.nicholson@aucklanduni.ac.nz

Keywords: *Geothermal model calibration, uncertainty quantification, ensemble-based methods, parameterisation, reservoir modelling.*

ABSTRACT

Computational reservoir models are commonly used to inform management decisions in the geothermal energy sector. With a well-calibrated model, a range of future scenarios can be simulated and informed decisions can be made. However, the task of calibrating large-scale geothermal models is challenging, both from a conceptual standpoint and in terms of computational cost. Furthermore, decision-makers typically desire the quantification of uncertainty and confidence in any calibration results. These problems have been addressed quite successfully in related fields, such as petroleum engineering, by using so-called ensemble-based uncertainty quantification methods.

Ensemble-based methods use a small collection (ensemble) of models, with each ensemble member having different values for the model parameters (such as deep mass and heat sources or subsurface permeabilities). The associated calibration methods guide this ensemble of different models to regions in parameter space which provide adequate matches to the measured field data, while ensuring an appropriate diversity of models to characterise uncertainty. In the Bayesian framework, ideally, the distribution of the ensemble should converge to the posterior probability distribution representing this uncertainty, i.e., the probability distribution of the unknown parameters given the measured field data.

A crucial task in ensemble methods, as well as in uncertainty quantification in general, is to simultaneously allow the parameters of interest to be uncertain and variable, while also being physically sensible (i.e., realistic). Careful parameterisations of the unknown parameters can fulfil these two objectives. In the context of ensemble-based methods, such parameterisations should also correspond to easy-to-evaluate prior terms. Here we propose a variety of possible parameterisations for deep mass and heat sources and subsurface permeabilities for use in the calibration of geothermal reservoir models. Each of the parameterisations presented can easily be implemented within an ensemble-based framework for model calibration.

1. INTRODUCTION

Computational modelling plays an important role in the management of a geothermal reservoir. Perhaps the most important attribute of a computational model is its ability to make accurate predictions. However, the accuracy of such predictions is naturally limited by, among other things, how well the computational model is calibrated. Calibration of a geothermal reservoir model generally entails estimation of controlling parameters such as the (anisotropic) permeability of the subsurface, and the locations and strengths of deep energy and mass up-flows.

The calibration process for real-world geothermal problems can be extremely time consuming however, due to the large number of parameters to be estimated and the computational cost of forward model simulations. Furthermore, decision-makers require quantification of the inherent uncertainty in any predictions made, which further increases the computational burden. Ensemble-based methods (Chen and Oliver, 2013; Emerick and Reynolds, 2013; Evensen et al., 2019) are computationally attractive tools for efficiently carrying out model calibration and uncertainty quantification for such large-scale models and have recently gained popularity in related areas such as petroleum engineering and hydrology.

Due to their ability to handle large numbers of parameters, ensemble methods can combine with more flexible and realistic parameterisation schemes than those used in standard geothermal calibration workflows. Traditionally, such calibration workflows involve adjusting a small number of unknown parameters and using fixed regions (e.g., zones or rock types) within which spatial model parameters are constant. Here we propose parameterisation schemes for use along with ensemble-based uncertainty estimation methods to characterize geothermal reservoirs better. The parameterisation methods considered include ways to generate bottom boundary mass- and heat-source distributions, and stratified permeability fields which are intersected by faults and dikes.

2. MODEL CALIBRATION AND UNCERTAINTY ESTIMATION

2.1 Calibration

The starting point for calibrating a model is defining the relationship between the measured field data, $\boldsymbol{d} \in \mathbb{R}^m$, the parameters to be estimated, $\boldsymbol{\theta} \in \mathbb{R}^n$, and any errors (or noise) corrupting the data, $\boldsymbol{e} \in \mathbb{R}^m$. A commonly used assumption is the additive error model, written

$$\boldsymbol{d} = \boldsymbol{f}(\boldsymbol{\theta}) + \boldsymbol{e}.$$

Here $\boldsymbol{f}: \mathbb{R}^n \to \mathbb{R}^m$ maps parameter inputs on to measured data and is typically referred to as the forward model. Here, it is the reservoir simulation model.

The goal of the calibration process is then to estimate the parameters, $\boldsymbol{\theta}$, based on matching the field data, $\boldsymbol{d}$. However, the properties of the forward model, and a lack of extensive data, lead to the estimation problem being (severely) ill-

ISSN 2703-4275

posed. To overcome this issue the estimation problem is typically either modified to include some type of regularisation or is formulated as a statistical inference problem. Here we adopt the latter approach, and use a Bayesian framework for statistical inference. Posing the problem in the Bayesian framework is particularly well-suited to incorporating and quantifying multiple sources of uncertainty and provides a natural setting for ensemble-based methods.

In the Bayesian framework, the solution to the inference problem is the posterior density, given by

$$p(\boldsymbol{\theta}|\boldsymbol{d}) \propto p(\boldsymbol{d}|\boldsymbol{\theta})p(\boldsymbol{\theta}),$$

where $p(\boldsymbol{d}|\boldsymbol{\theta})$ is the likelihood function, and $p(\boldsymbol{\theta})$ is the prior density, which encodes any prior beliefs about the parameters. Assuming that the errors are distributed normally, with mean $\mathbf{0}$ and covariance $\boldsymbol{C_e}$, i.e., $\boldsymbol{e}\sim p(\boldsymbol{e}) = \mathbf{N}(\mathbf{0}, \boldsymbol{C_e})$, and that the prior density is also Gaussian, $p(\boldsymbol{\theta}) = \mathbf{N}(\boldsymbol{\theta}_*, \boldsymbol{C_\theta})$, the posterior is then

$$p(\boldsymbol{\theta}|\boldsymbol{d}) \propto \exp\left\{-\frac{1}{2}(\|\boldsymbol{L}_e(\boldsymbol{d}-\boldsymbol{f}(\boldsymbol{\theta}))\|^2 + \|\boldsymbol{L}_\theta(\boldsymbol{\theta}-\boldsymbol{\theta}_*)\|^2)\right\},$$

where $\boldsymbol{L}_e^T\boldsymbol{L}_e = \boldsymbol{C}_e^{-1}$ and $\boldsymbol{L}_\theta^T\boldsymbol{L}_\theta = \boldsymbol{C}_\theta^{-1}$.

Although the posterior is easily written down, when $\boldsymbol{f}$ is nonlinear, as is the case for geothermal models, generating samples from it is notoriously costly. The gold standard is to employ Markov chain Monte Carlo (MCMC) methods, though in the geothermal setting these can easily lead to run times of more than a month (Cui, Fox, and O'Sullivan, 2011, 2019). Ensemble-based methods result in samples from an approximate posterior, at a vastly reduced computational cost.

2.2 Ensemble-based methods

There are a variety of ensemble-based methods which can be used for calibration. The approach of Chen and Oliver (2013) is particularly robust and has the advantage of being essentially derivative-free, i.e., requires no explicit derivative information. The approach is based largely on the randomised-maximum-likelihood (RML) approach (Oliver, He, and Reynolds, 1996), with an ensemble approximation to the sensitivity matrix.

The end goal is the generation of an ensemble of $s \in \mathbb{N}$ samples, $\boldsymbol{\theta}_1, \boldsymbol{\theta}_2, \dots, \boldsymbol{\theta}_s$, from the posterior parameter distribution. This goal is achieved via the iterative updating of an ensemble of samples initially drawn from the prior, $\boldsymbol{\theta}_1^0, \boldsymbol{\theta}_2^0, \dots, \boldsymbol{\theta}_s^0$. Specifically, letting $\boldsymbol{\Theta}^i = [\boldsymbol{\theta}_1^i, \boldsymbol{\theta}_2^i, \dots, \boldsymbol{\theta}_s^i]$, where $i = 0,1,\dots,q \in \mathbb{N}$ is the iteration number, $\boldsymbol{F}^i = [\boldsymbol{f}(\boldsymbol{\theta}_1^i), \boldsymbol{f}(\boldsymbol{\theta}_2^i), \dots, \boldsymbol{f}(\boldsymbol{\theta}_s^i)]$, and $\boldsymbol{D} = [\boldsymbol{d}+\boldsymbol{e}_1, \boldsymbol{d}+\boldsymbol{e}_2, \dots, \boldsymbol{d}+\boldsymbol{e}_s]$, where $\boldsymbol{e}_i\sim p(\boldsymbol{e})$, the update of the parameters from iteration i to iteration $i+1$ is given by

$$\boldsymbol{\Theta}^{i+1} = \boldsymbol{\Theta}^i - \left(\boldsymbol{J}^T\boldsymbol{C}_e^{-1}\boldsymbol{J} + \boldsymbol{C}_\theta^{-1}\right)^{-1}\left(\boldsymbol{J}^T\boldsymbol{C}_e^{-1}(\boldsymbol{F}-\boldsymbol{D}) + \boldsymbol{C}_\theta^{-1}\left(\boldsymbol{\Theta}^i - \boldsymbol{\Theta}^0\right)\right),$$

where $\boldsymbol{J}$ is the empirical ensemble Jacobian matrix, defined as

$$\boldsymbol{J} = \left(\boldsymbol{F}^i - \overline{\boldsymbol{F}}^{\boldsymbol{i}}\right)\left(\boldsymbol{\Theta}^i - \overline{\boldsymbol{\Theta}}^{\boldsymbol{i}}\right)^{-1}.$$

Here $\overline{\boldsymbol{F}}^{\boldsymbol{i}} \in \mathbb{R}^{m\times s}$ and $\overline{\boldsymbol{\Theta}}^{\boldsymbol{i}} \in \mathbb{R}^{n\times s}$ are the matrices comprised of the means of the simulation ensemble and parameter ensemble at iteration i, respectively, i.e.,

$$\overline{\boldsymbol{F}}^{\boldsymbol{i}} = (\boldsymbol{F}^i\mathbf{1}/\boldsymbol{s})\mathbf{1}^T, \quad \overline{\boldsymbol{\Theta}}^{\boldsymbol{i}} = (\boldsymbol{\Theta}^i\mathbf{1}/\boldsymbol{s})\mathbf{1}^T,$$

where $\mathbf{1} \in \mathbb{R}^{s\times 1}$ is a column vector of 1's. It is worth noting that the matrix $\left(\boldsymbol{\Theta}^i - \overline{\boldsymbol{\Theta}}^{\boldsymbol{i}}\right)$ is generally singular, and thus a pseudoinverse is taken, as explained by, for example, Chen and Oliver (2013).

Key to success of the ensemble-based approach is the choice of representations (or parameterisations) of the unknowns, such as subsurface permeability and deep mass and heat sources. We next consider various representations which could prove successful in the geothermal model calibration setting.

3. REPRESENTING UNKNOWN PARAMETERS

3.1 Preliminaries

Without any restrictions, choices for representing unknown parameters are fairly arbitrary. However, in order to maintain some formal mathematical foundations, and for computational ease, we restrict our representations to Gaussian densities, $\mathbf{N}(\boldsymbol{\theta}_*, \boldsymbol{C}_\theta)$, along with some additional filtering of the associated samples generated from these. These densities are defined by a mean, $\boldsymbol{\theta}_*$, and covariance matrix, $\boldsymbol{C}_\theta$. Though this constraint may appear limiting or overly restrictive, as explained below it is possible to encode fairly arbitrary structures and varying levels of smoothness through the use of Gaussian densities, and thus allow for samples of physically reasonable parameters. Most of the prior parameter sampling schemes used here are based on Matérn class covariance matrices (see (Roininen, Huttunen, and Lasanen, 2014) and the references therein), which easily encode various degrees of smoothness and structure.

We consider the representation of deep sources of mass or energy, subsurface permeability, and faults and intrusions. The deep sources are two-dimensional (defined on the bottom boundary of the computational domain), while the permeability distribution is three-dimensional (defined throughout the computational domain shown in Figure 1).

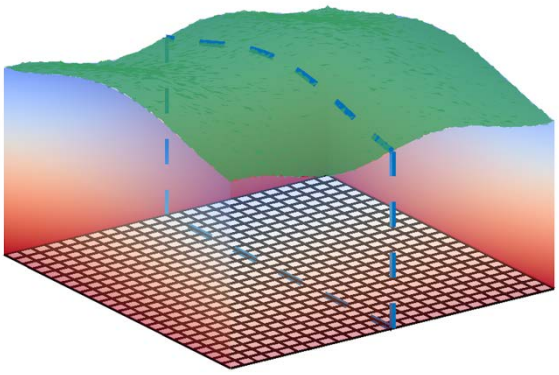

Figure 1: Schematic of the computational domain used for examples. Deep sources are defined on the bottom boundary and permeability is defined throughout (blue dashed line shows a vertical cross-section used for Figures 8-11).

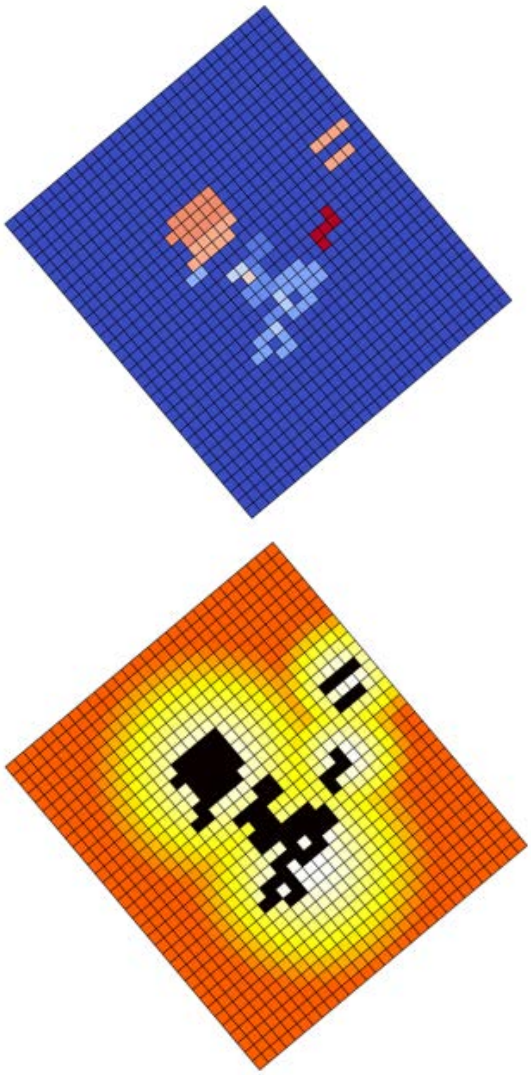

Figure 2: Bottom mass flows (top) and conductive heat fluxes (bottom) for a Wairakei geothermal field model (considered in (Bjarkason et al., 2019)). Dark blue indicates no mass flow, while black indicates no conductive heat flux.

3.2 A reference real-world reservoir model

The overarching goal of the representations considered here is to be able to generate physically sensible parameters, while simultaneously enabling enough parameter flexibility to match observations and enough parameter variability to provide a reasonable reflection of the true uncertainty. Standard representations of unknown model parameters typically found in the literature use fairly simple and fixed geometries for bottom upflows and permeabilities, as shown in Figures 2 and 3. For instance, the permeability distribution in a model is commonly parameterised using a small number of rock-types or zones, where the permeability is constant within each zone. When employing automatic calibration methods, the extent or edges of these zones are usually fixed. It is unlikely, however, that the unknowns are so simple, and such representations can easily lead to difficulty in fitting measured field data. Therefore, when manually calibrating models, it is common to iteratively redefine or split up zones to achieve better matches to data. Furthermore, limiting the representation of the unknowns to such simple geometries introduces so-called modelling errors, something calibration techniques handle particularly poorly, see for example (Kaipio and Somersalo, 2007; Maclaren et al., 2020).

For reference, we consider a model of the Wairakei geothermal system Wairakei, New Zealand, which was considered by Bjarkason et al. (2019) and is based on a model developed by Yeh et al. (2016). Figure 2 shows the bottom mass flows and heat fluxes in the model, and Figure 3 presents a vertical cross-section of the subsurface permeability.

This Wairakei model is a result of years of model development starting from very coarse models early on and gradually introducing refinement as computational resources improved and more data became available during field development (O'Sullivan, Yeh, and Mannington, 2009; Yeh et al., 2016). The Wairakei model presents a state-of-the-art model, which has relatively complex structural features. Most other geothermal models used to describe other fields, which have been developed based on shorter observation histories and therefore sparser field data, tend to have simpler model structures than the model displayed in Figures 2 and 3.

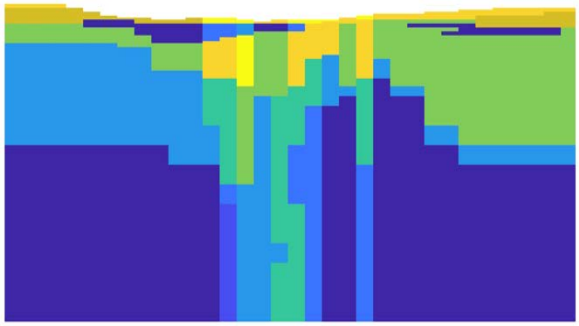

Figure 3: Vertical cross-section of subsurface permeability for a Wairakei geothermal field model (considered in (Bjarkason et al., 2019)).

As shown in Figure 2, the bottom boundary has a small number of mass upflow zones and most of the boundary area has zero mass flux (dark blue area). The conductive heat flux varies smoothly across most of the boundary, apart from areas associated with upward mass flux where the conductive heat fluxes were set to be zero. Figure 3 illustrates the model permeabilities along a vertical cross-section. The permeability distribution shows layered zones, which are most clearly visible on the flanks of Figure 3 and reflect the understanding of the lithological structure at Wairakei. The centre of Figure 3 displays vertical fault-like features, some of which may represent expected or estimated locations of faults and may also reflect areas where the permeability structure needed to be refined to improve model calibration.

In the following three subsections we illustrate, through displaying multiple samples, various representations which can capture different features of the bottom boundary sources and subsurface permeability. We begin by discussing several representations for deep sources, of mass or energy, and then move on to parameterisations of the subsurface permeability and faults and intrusions.

3.3 Representations for deep sources

3.3.1 Heat fluxes

As shown in Figure 2, the bottom heat-flux distribution is taken to be fairly smooth (away from areas where the mass flows are assigned nonzero values). This is our starting point for representing the deep upflows. Gaussian priors are well suited to describing spatially smooth distributions (that is, spatially correlated parameter fields) and may, therefore, be appropriate for describing prior ideas for conductive heat-flux boundary conditions (like the ones shown in the lower plot in Figure 2).

In Figure 4, we show four samples from a Gaussian prior having essentially no structure other than favouring fairly smooth samples. For an appropriately chosen smoothness, we can get boundary heat-flux samples which resemble the smooth heat flux features in Figure 2 (see lower subplots in Figure 4). In principle, positive background heat fluxes can be assigned in this way over the whole bottom boundary, although ensuring positivity may require additional parameter truncation or transformation. Moreover, if preferred, zero conductive heat fluxes can also be enforced in areas having nonzero mass flows (as is the case for the Wairakei model boundary conditions in Figure 2), which are considered in the following subsection. Again, this may require truncation of the Gaussian samples.

3.3.2 Mass fluxes

For mass-flux bottom boundary conditions, one could consider directly applying a spatially smooth Gaussian prior like the one discussed for conductive heat fluxes. However, a possible drawback to such a representation is that it can result in positive mass fluxes (inflow of mass) across essentially the entire bottom boundary of the computational domain. Such a scenario would not represent physically realistic boundary conditions. Alternatively, such Gaussian priors could result in both positive and negative boundary mass fluxes. Although negative (downward) mass fluxes are expected to appear when considering arbitrary horizontal cross-sections in real geothermal reservoirs, especially for a cross section that a model bottom boundary usually represents (which for practical reasons is typically placed far above the roots (heat sources) of the geothermal system), it is standard practice to only include zones of upward (positive) mass flow at the bottom boundary as shown in Figure 2.

There are several possible ways to generate prior samples which only have nonnegative mass fluxes, including the use of so-called level sets (Xie, Efendiev, and Datta-Gupta, 2011; Chang, Zhang, and Lu, 2010) or truncated Gaussian prior models (Oliver and Chen, 2018), where values below (or above) some threshold are set to a fixed value. Figure 5 shows how a level-set approach, which assigns zero mass fluxes to areas where the fluxes are below a certain threshold, can produce distributions which resemble the mass-flow boundary condition displayed in Figure 2.

It may often be preferable to have the deep upflows near the centre of the domain. This can easily be encoded by adapting the variance accordingly over the bottom boundary. In Figure 6, we show four samples generated by reducing the variance towards the edges of the basal domain; we also increase the smoothness for the samples and implement the level-set approach. This type of approach may be appealing for models where the geothermal reservoir is believed to be close to the centre of the model domain and the model edges (that is, the horizontal boundaries) of the model extend far away to reduce the influence of the side boundary conditions.

Finally, we note that various other features can be encoded. For example, sources of mass and energy may be related to fractures and/or intrusive bodies such as dikes (see, e.g., Figures 2 and 3, and (Gunnarsson and Aradóttir, 2015)). Such objects can be represented, for instance, by elongated features. Elongated shapes on the bottom boundary can be generated by assigning an anisotropic spatial correlation for the prior Gaussian samples. This results in Gaussian features which are stretched along a dominant direction along which the basal parameters are more correlated. However, more general shapes can also be considered. For example, in various geophysical settings it is desirable to be able to generate samples with channel-like geometries, like those shown in Figure 7, which were also generated using a Gaussian prior.

3.4 Representations for subsurface permeability

3.4.1 Stratified permeability distributions

The Gaussian representations proposed here for the deep upflows can also be generalized to three dimensions and used for describing subsurface permeability. However, subsurface permeability typically exhibits a layer-like structure, as shown in Figure 3, and thus we focus on representations which promote such structure. Here we present depictions of permeabilities along vertical slices (like the one marked by the blue dashed line in Figure 1). Though we do not show it here, the sampled permeability distributions can have a complex three-dimensional structure. For example, sampled permeabilities along horizontal cross sections may look like some of the distributions discussed in the subsections of Section 2.

In Figure 8, we show four samples generated using an anisotropic Matérn class covariance matrix, with a longer correlation length in the horizontal direction than in the vertical direction. Furthermore, by again applying the level-set method, we can generate permeability samples appearing to be partitioned into different rock types, as is standard in the geothermal community. The permeability samples shown in Figure 8 portray structure which looks similar to the lithological structure on the flanks of Figure 3.

The layered stratigraphy can easily be generalized to accommodate tilted geological structure, as shown in Figure 9. Furthermore, by not carrying out the level-set transformation, we can generate smoothly varying samples, still displaying the layer-like structure, as shown in Figure 10. The samples shown in Figures 8–10 were generated by using a homogeneous prior mean over the vertical slice. However, if prior knowledge suggests otherwise, the prior mean can vary over the model domain. For instance, on average, we can expect permeability to decrease with increasing depth, which we can accommodate by choosing a prior mean which decreases accordingly with depth.

Notably, the parameterisations discussed here for subsurface permeability do not require the knowledge of the location of the boundaries of facies a priori, something which is typically needed with standard approaches. Having flexible facies boundaries could help to achieve acceptable matches to observations and allow for greater posterior parameter

ISSN 2703-4275

variability, which may result in more reliable uncertainty estimates.

3.4.2 Representations for faults and intrusions

Finally, we briefly discuss the representation of faults and intrusions, such as dikes. In the middle of Figure 2, vertical fault-like structures are evident. In practice, faults are commonly assumed to follow fairly simple linear shapes. Such features can also be generated using Gaussian distributions. Specifically, the locations and slopes of faults can be easily sampled, see Figure 11. Lithological units are commonly displaced or offset along faults, as seen, for example, in graben and horst. The first three samples in Figure 11 display strata which are offset along linear faults. However, offsets need not be restricted to linear structures, as the bottom right example shows in Figure 11.

However, more complex, and arguably more natural geometries can also be generated in a straightforward manner by considering the faults as samples from a Gaussian distribution. Figure 12 displays more complex random samples of sheet-like structures, which could be used to represent faults or dikes. Formation permeabilities could be modified along such planar structures to generate features such as the vertical ones in the centre of Figure 3.

Lastly, the generation of other intrusive bodies can also be placed into this framework. Rather arbitrary shapes can be generated to describe intrusive bodies. As an example, the slope, location, depth, and radius of a cylindrically shaped intrusive can be randomly generated, see Figure 13.

4. CONCLUSION

In this paper we have considered various stochastic representations for several unknown parameters which are often estimated when carrying out geothermal model calibration. The representations give qualitatively very different samples, though all are based largely on Gaussian distributions. This ensures any of the representations chosen can easily be used within ensemble-based methods, which can then be used to efficiently estimate parameter uncertainty. Furthermore, we demonstrated that Gaussian distributions can be used to generate prior parameter samples which have features which resemble both what we might expect for geothermal settings and parameter choices commonly used in standard geothermal models. However, the types of parameterisation schemes proposed here could prove to be more flexible and useful than standard geothermal parameterisation schemes.

ACKNOWLEDGEMENTS

Part of this work was carried out under the Collaborative Research Project of the Institute of Fluid Science, Tohoku University. This work was partially supported by Landsvirkjun, the National Power Company of Iceland.

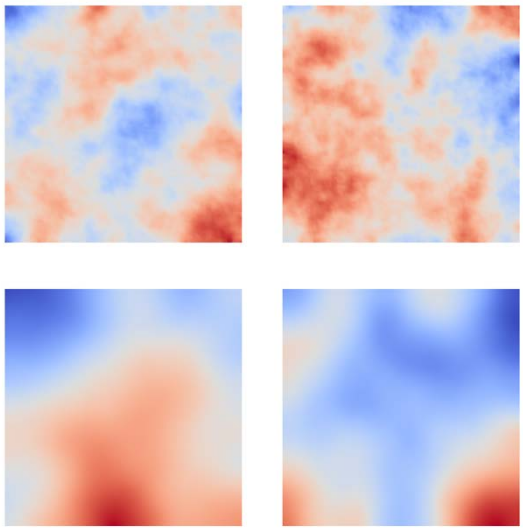

Figure 4: Four deep upflow samples generated using a Gaussian distribution which promotes smoothness. The lower row shows samples drawn from a smoother prior distribution than that used for the samples in the top row.

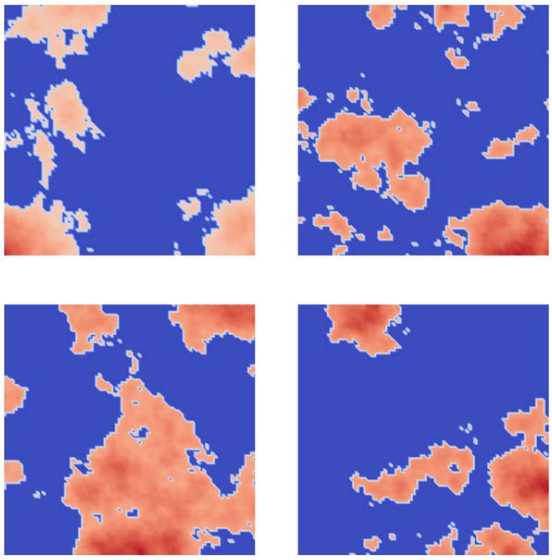

Figure 5: Four deep upflow samples generated using a Gaussian distribution which promotes smoothness and the application of a level-set method.

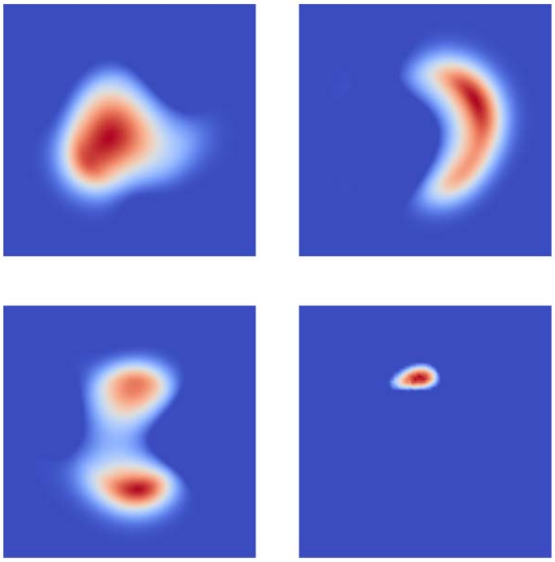

Figure 6: Four deep upflow samples generated by using a Gaussian distribution which promotes a high order of smoothness, applying a level-set method, and using a spatially varying variance which decays toward the model edges.

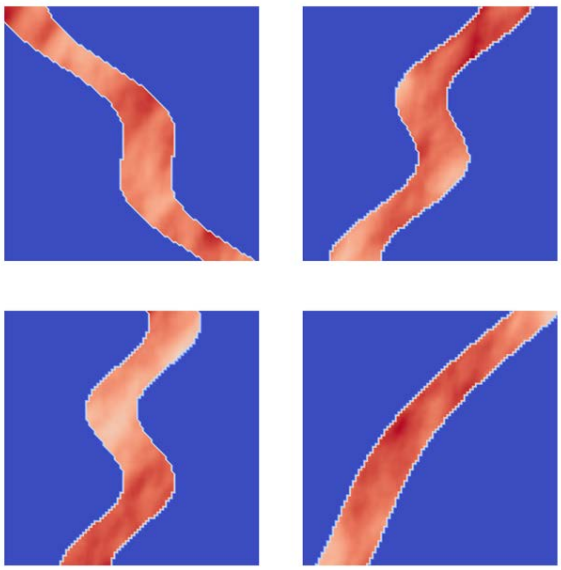

Figure 7: Four deep upflow samples generated using a Gaussian distribution which generates heterogeneous channel-like structures.

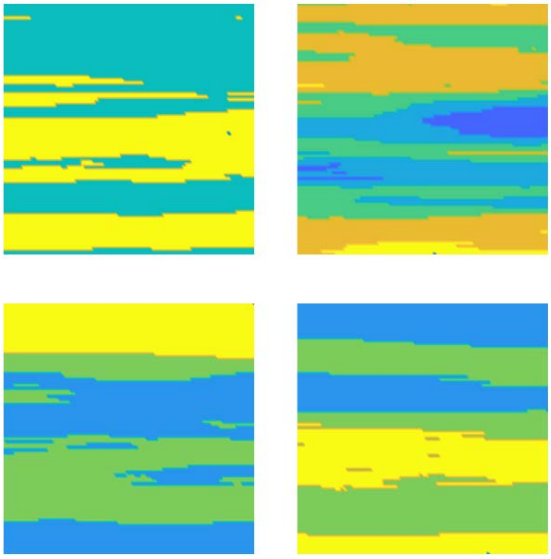

Figure 8: Four subsurface permeability samples generated using an anisotropic Gaussian distribution which promotes longer correlation in the horizontal direction, and the application of a level-set method to give large homogeneous rock types.

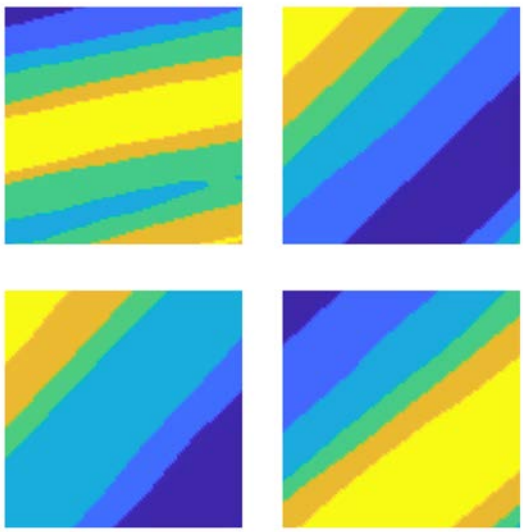

Figure 9: Four subsurface permeability samples, similar to those in Figure 8, but with different level sets and with the addition of tilt.

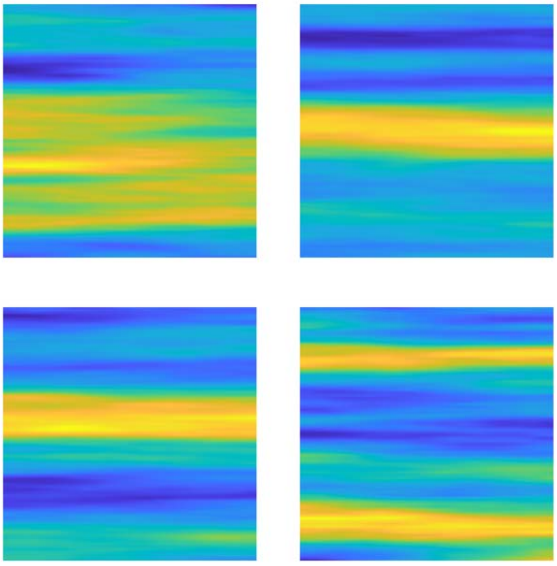

Figure 10: Four subsurface permeability samples generated using an anisotropic Gaussian distribution which promotes longer correlation in the horizontal direction.

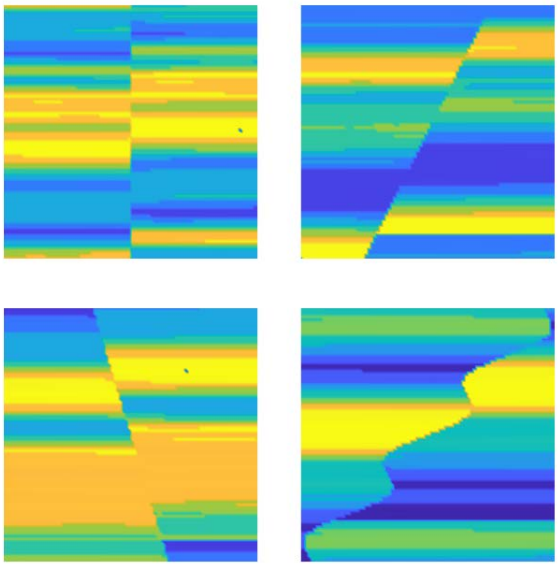

Figure 11: Four simple fault samples where stratified permeability samples are offset along the sampled faults.

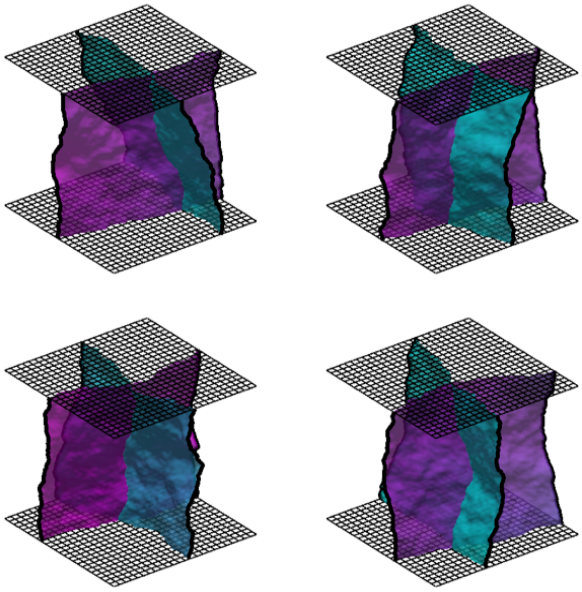

Figure 12: Four samples of more complex faults or dikes.

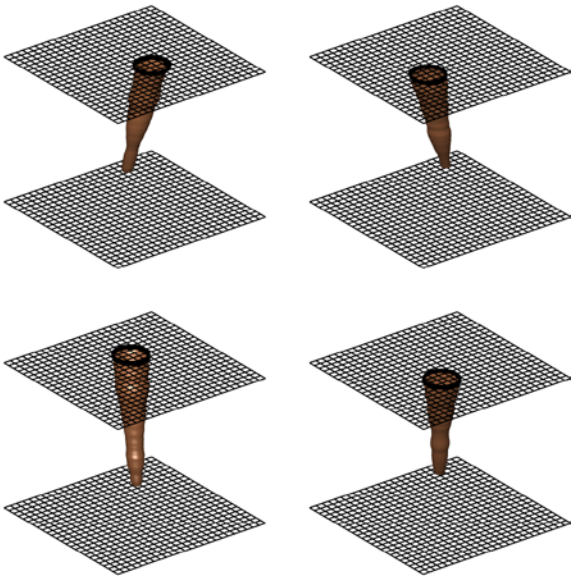

Figure 13: Four samples of cylindrical intrusions.

REFERENCES

Bjarkason, E.K., Yeh, A., O'Sullivan, J.P., Croucher, A., O'Sullivan, M.J.: Non-uniqueness of geothermal natural-state simulations. *Proc. 41st New Zealand Geothermal Workshop*, Auckland, New Zealand. (2019).

Chang, H., Zhang, D., Lu, Z.: History matching of facies distribution with the EnKF and level set parameterization. *Journal of Computational Physics*, *229*(20), 8011–8030. (2010).

Chen, Y., Oliver, D.S.: Levenberg–Marquardt forms of the iterative ensemble smoother for efficient history matching and uncertainty quantification. *Computational Geosciences*, *17*(4), 689–703. (2013).

Cui, T., Fox, C., O'Sullivan, M.J.: Bayesian calibration of a large-scale geothermal reservoir model by a new adaptive delayed acceptance Metropolis Hastings algorithm. *Water Resources Research*, *47*(10). (2011).

Cui, T., Fox, C., O'Sullivan, M.J.: A posteriori stochastic correction of reduced models in delayed- acceptance MCMC, with application to multiphase subsurface inverse problems. *International Journal for Numerical Methods in Engineering*, *118*(10), 578–605. (2019).

Emerick, A.A., Reynolds, A.C.: Ensemble smoother with multiple data assimilation. *Computers & Geosciences*, 55, 3–15. (2013).

Evensen, G., Raanes, P.N., Stordal, A.S., Hove, J.: Efficient implementation of an iterative ensemble smoother for big-data assimilation and reservoir history matching. *Frontiers in Applied Mathematics and Statistics*, *5*, 47. (2019).

Gunnarsson, G., Aradóttir, E.S.P.: The deep roots of geothermal systems in volcanic areas: Boundary conditions and heat sources in reservoir modeling. *Transport in Porous Media*, *108*(1), 43–59. (2015).

Kaipio, J., Somersalo, E.: Statistical inverse problems: discretization, model reduction and inverse crimes. *Journal of computational and applied mathematics*, *198*(2), 493–504. (2007).

Maclaren, O.J., Nicholson, R., Bjarkason, E.K., O'Sullivan, J.P., O'Sullivan, M.J.: Incorporating posterior-informed approximation errors into a hierarchical framework to facilitate out-of-the-box MCMC sampling for geothermal inverse problems and uncertainty quantification. *Water Resources Research*, *56*(1). (2020).

Oliver, D.S., Chen, Y.: Data assimilation in truncated plurigaussian models: impact of the truncation map. *Mathematical Geosciences*, *50*(8), 867–893. (2018).

Oliver, D.S., He, N., Reynolds, A.C.: Conditioning permeability fields to pressure data. In *ECMOR V-5th European conference on the mathematics of oil recovery*, Leoben, Austria. (1996).

O'Sullivan, M.J., Yeh, A., Mannington, W.I.: A history of numerical modelling of the Wairakei geothermal field. *Geothermics*, *38*(1), 155–168. (2009).

Roininen, L., Huttunen, J.M., Lasanen, S.: Whittle-Matérn priors for Bayesian statistical inversion with applications in electrical impedance tomography. *Inverse Problems & Imaging*, *8*(2), 561–568. (2014).

Xie, J., Efendiev, Y., Datta-Gupta, A.: Uncertainty quantification in history matching of channelized reservoirs using Markov chain level set approaches. In *SPE Reservoir Simulation Symposium.* Society of Petroleum Engineers. (2011).

Yeh, A., O'Sullivan, M.J., Newson, J.A., Mannington, W.I.: Use of PEST for improving a computer model of Wairakei-Tauhara. *Proc. 38th New Zealand Geothermal Workshop*, Auckland, New Zealand. (2016).

ISSN 2703-4275